standard-deviation contours. From our Monte Carlo study, we conclude the probability of obtaining a value of $(x^2+y^2)^{1/2} \geq 0.5$ is 25% in an event sample of this size. We therefore have no evidence that either x or y is different from zero. This is consistent with the results of the previous experiments.[6–9]

If we now assume the final state of the decay is the symmetric $I=1$ state, then the decay only depends on the parameter y. Under that assumption we obtain

$$y=-0.66\pm0.27\,,$$

where the error includes the statistical uncertainty in $\Gamma_L(3\pi)$. A systematic shift in the value of $\Gamma_L(3\pi)$ of $0.1\times10^6\ \text{sec}^{-1}$ would change y by about 0.1.

Since our result is consistent with $x=y=0$, we can calculate $\Gamma_L(3\pi)$ assuming the observed events are due entirely to $K_L{}^0 \to \pi^+\pi^-\pi^0$. We find $\Gamma_L(3\pi)=(2.71\pm0.28)\times10^6\ \text{sec}^{-1}$, which is in excellent agreement with the value obtained by Budagov *et al.*[12] The π^0 kinetic-energy spectrum in the K^0 rest frame is shown in Fig. 3. Variation in the detection efficiency as a function of π^0 energy is negligible. The straight line drawn is from a fit using the matrix element squared:

$$|M|^2 \sim 1+2\alpha(M_K/M_\pi{}^2)(2T_{\pi^0}-T_{\max})\,.$$

We find $\alpha=-0.26\pm0.07$, which agrees with the known slope of the K_L decay, $\alpha=-0.20\pm0.014$.[1]

ACKNOWLEDGMENTS

We thank Dr. N. P. Samios for his generous support and Professor L. Wolfenstein for helpful conversations. We acknowledge the careful data handling by Mrs. V. Austen and Mrs. A. Maxwell. We also wish to thank our scanners, measurers, and the crew of the 30-in. bubble chamber for their efforts.

PHYSICAL REVIEW D VOLUME 3, NUMBER 7 1 APRIL 1971

Double-Regge-Pole Description of the Reaction $K^-n \to K^-\pi^-p$ at 5.5 GeV/c*

Y. Cho, M. Derrick, D. Johnson,† B. Musgrave, T. Wangler, and J. Wong
Argonne National Laboratory, Argonne, Illinois 60439

and

R. Ammar, R. Davis, W. Kropac, and H. Yarger
University of Kansas, Lawrence, Kansas 66044

and

B. Werner‡
Northwestern University, Evanston, Illinois 60201

(Received 12 October 1970)

New data on the reaction $K^-d \to K^-\pi^-pp_s$ at 5.5 GeV/c are presented. The experimental distributions are analyzed in terms of a double-peripheral Regge-pole model. The events were assigned to two dominant diagrams using the Van Hove angle. These diagrams, involving Pomeranchuk and meson exchanges, provide a good description of the reaction without additional form factors of the momentum transfer.

I. INTRODUCTION

In recent years the extension of the Regge-pole model from two-body and quasi-two-body reactions to reactions involving many particles has been studied by several groups.[1–7] In particular, the double-Regge-pole model (DRM) has been successful in describing many three-body final states. Because the Regge model was originally introduced as an asymptotic expansion, some of these fits were restricted to the relatively small fraction of events where all two-particle subenergies were larger than some prescribed limits. Berger[3] extended the model down to the threshold of one of the two-body subenergies involved and obtained satisfactory descriptions of several reactions.

Cuts in the subenergies can also provide a mechanism for selecting events appropriate to the different peripheral diagrams. This is not a unique method of selection, and Alexander *et al.*[4] used the four-momentum transfers at the beam and target vertices. Recently, Van Hove[8]

* Work supported by the U. S. Atomic Energy Commission and by the National Science Foundation.

† ANL Predoctoral Fellow from the University of Kansas, Lawrence, Kan.

‡ Present address: University of Rochester, Rochester, N. Y.

[1] Chan Hong-Mo *et al.*, Nuovo Cimento **49**, 157 (1967); **51**, 696 (1967).

[2] E. Berger, Phys. Rev. Letters **21**, 701 (1968).

[3] E. Berger, Phys. Rev. **166**, 1525 (1968); **179**, 1567 (1969).

[4] G. Alexander *et al.*, Phys. Rev. **177**, 2092 (1969).

[5] M. L. Ioffredo *et al.*, Phys. Rev. Letters **21**, 1212 (1968).

[6] J. Andrews *et al.*, Phys. Rev. Letters **22**, 731 (1969).

[7] M. S. Farber *et al.*, Phys. Rev. Letters **22**, 1394 (1969).

[8] L. Van Hove, Nucl. Phys. **B9**, 331 (1969).

has proposed the use of longitudinal phase-space plots in order to associate the kinematics and the dynamics of reactions without introducing cuts in the subenergies.

In this experiment, we studied the reaction $K^-n \to K^-\pi^-p$ at 5.5 GeV/c, and attempted to describe the reaction in detail using a DRM in conjunction with the Van Hove plot.

II. EXPERIMENTAL DATA

The events used were obtained from a 5-event/μb exposure of the 30-in. deuterium bubble chamber to a 5.5-GeV/c K^- beam at the ZGS. The film was scanned for three- and four-prong events. In selecting four-prong events, one of the positive tracks was required to end in the chamber. All of the four-prong events were measured on conventional digitizers, and about 75% of the three-prong events were measured using POLLY II.[9] The remaining three-prong events were not measured. All the quantities used in this paper are corrected for this loss. The events were then spatially reconstructed and kinematically fitted to the possible final-state hypotheses. For the three-prong events, the bubble densities of tracks were measured by POLLY and compared with those expected from the kinematic fits during the fitting process. The consistency of bubble density for the four-prong events was checked by physicists.

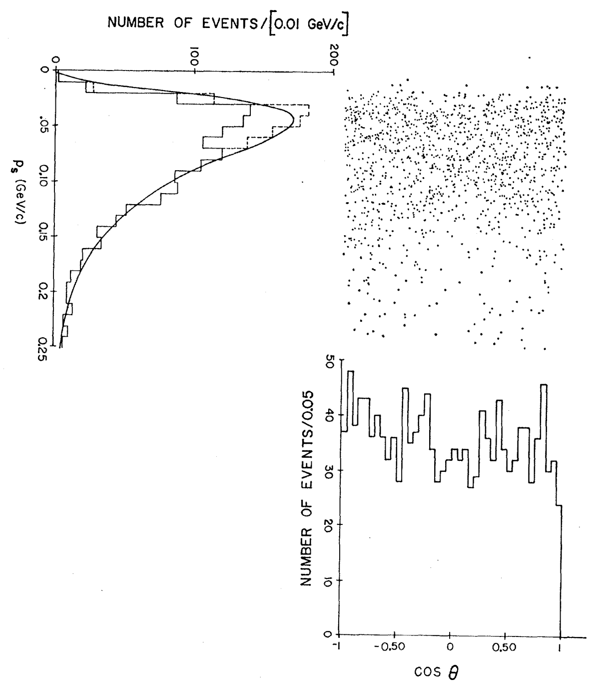

FIG. 1. Cos$\theta_{\rm lab}$ vs p_s distribution for the spectator. The solid line in the p_s distribution shows the Hulthén distribution, and the dashed histogram includes the correction for unmeasured three-prong events.

[9] W. W. H. Allison *et al.*, Nucl. Instr. Methods **79**, 341 (1970).

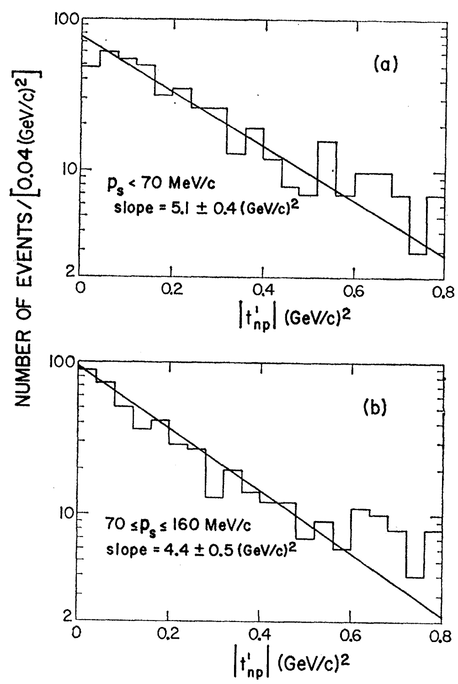

FIG. 2. Momentum transfer from initial to final nucleon for $(t_{np}'=|t_{np}-t_{\rm min}|)$. (a) $p_s<70$ MeV/c and (b) $70\leqslant p_s\leqslant 160$ MeV/c. The fit to a straight line was made for events with $t'<0.45$ (GeV/c)^2.

More detailed discussion of the data reduction is given elsewhere.[10]

We assign some 1300 events to the reaction

$$K^-d \to K^-\pi^-pp_s\,, \tag{1}$$

where p_s denotes the spectator proton. The ratio of visible spectator (four-prong) events to invisible spectator (three-prong) events was 0.91 for the sample of film completely measured. The slower proton in the final state was called the spectator, thus introducing a bias in the nucleon momentum transfer distribution. In order to minimize the effect of this bias, we have used only those events where the spectator momentum was less than 160 MeV/c.

If our designation of the spectator is correct, then its angular distribution should be isotropic and its momentum distribution should agree with the Hulthén distribution. We define θ as the angle between the incident K^- and the outgoing spectator in the laboratory system. Figure 1 shows a scatter plot of cosθ as a function of the spectator momentum p_s. An isotropic angular distribution, independent of spectator momentum, is clearly shown, and the projection of the scatter plot onto the p_s axis shows that the spectator momentum distribution agrees well with the Hulthén distribution. From this we conclude that our choice of the spectator is statistically correct.

[10] B. Werner, thesis, Northwestern University, 1969 (unpublished).

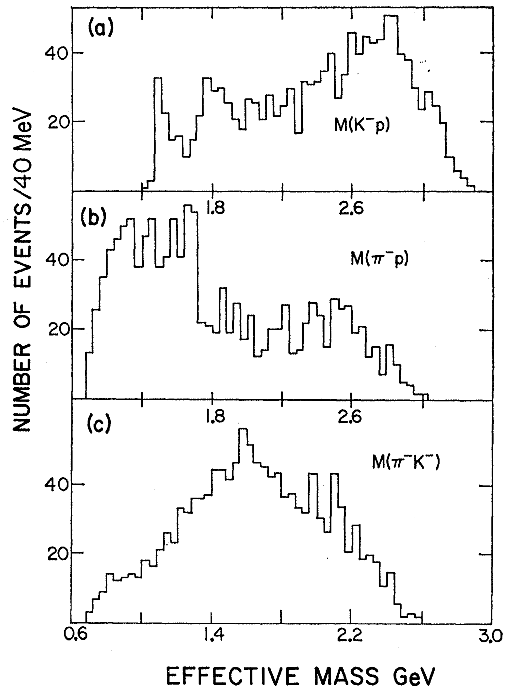

FIG. 3. Distributions of two-body subenergies. (a) $M(K^-p)$, (b) $M(\pi^-p)$, and (c) $M(\pi^-K^-)$.

The suppression in the forward direction due to the Pauli exclusion principle can be seen in the momentum transfer distributions of Fig. 2. Figure 2(a) shows the t_{np}' distribution $|t_{np}'|=|t_{np}-t_{\min}|$ for the events with spectator momentum $p_s<70$ MeV/c. Figure 2(b) shows this distribution for $70\leqslant p_s\leqslant 160$ MeV/c. The effect of the exclusion principle is clearly seen in the low momentum spectator events of Fig. 2(a). In the subsequent analysis, a correction was made for each t_{np} bin using a factor derived from the t_{np} distributions for the two intervals of spectator momentum.

While the final-state protons, being slow in the laboratory system, were easily identified, about 25% of the events were kinematically ambiguous to the $K^-\pi^-$ interchange. These ambiguous events were assigned to the hypothesis with lower χ^2. Although this criterion could introduce some contamination in the sample, the effect was found to be unimportant.[11]

The K^-p mass spectrum of Fig. 3(a) shows weak production of $Y^{*0}(1520)$ and $Y^{*0}(1820)$. The lack of resonance production in the π^-p combination is equally evident in Fig. 3(b). The broad enhancement near threshold of the π^-p subenergy is a feature of multiperipheral interactions. Figure 3(c) shows the $K^-\pi^-$ mass spectrum.[12]

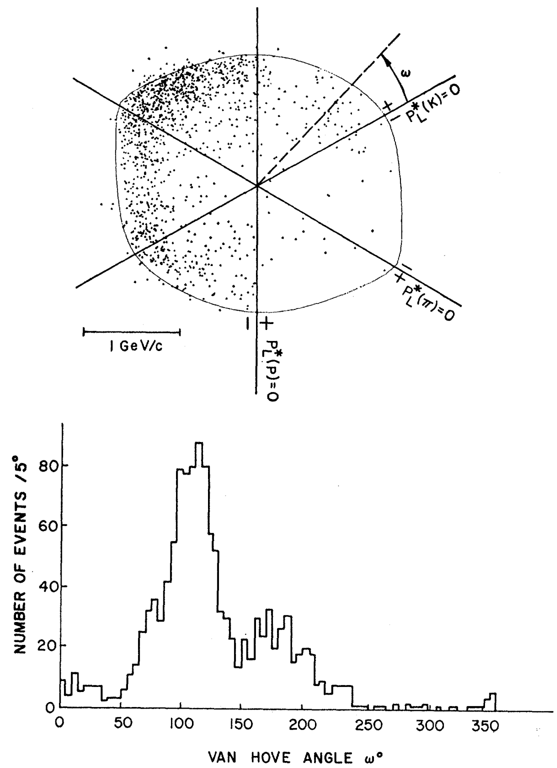

FIG. 4. (a) The Van Hove plot and (b) its projection onto the ω axis. The origin of the ω scale is shown in (a).

The Van Hove plot, and its projection shown in Fig. 4, indicates the dominance of two groups of events arising from two processes. These are (1) the large number of events clustered around the Van Hove angle, $\omega=120°$, involving a fast forward K^-, a slow π^-, and a fast backward proton in the production c.m. system, and (2) the small group of events around $\omega=180°$ having a forward π^-, a slow K^-, and a backward proton in the over-all c.m. system. These features suggest the importance of the two peripheral-production mechanisms shown schematically in Fig. 5. There is no contribution from the baryon exchange. The details are discussed in Sec. III.

III. DOUBLE-REGGE-POLE MODEL

The model used in this analysis involves Figs. 5(a) and 5(b) for which amplitudes are written[13]

$$M_a=C_aG_\pi(t_{np})(S_{p\pi}/S_{20})^{\alpha_\pi}G(t_{np},t_{KK},\omega_{Ta})\times(S_{K\pi}/S_{10})^{\alpha_P}G_P(t_{KK}),\quad(2a)$$

$$M_b=C_bG_\pi(t_{np})(S_{Kp}/S_{20})^{\alpha_\pi}G(t_{np},t_{K\pi},\omega_{Tb})\times(S_{K\pi}/S_{10})^{\alpha_{K^*}}G_{K^*}(t_{K\pi}).\quad(2b)$$

[11] We studied the effect of this ambiguity by two methods of event selection, one by assigning the event to the lower-χ^2 hypothesis, and the other by giving equal weight of 0.5 to events of both hypotheses.

[12] The events have been used to measure the $T=\frac{3}{2}$ elastic cross section by a Chew-Low extrapolation. Y. Cho *et al.*, Phys. Letters **32B**, 409 (1970).

[13] The kinematic variables for the reaction $K^-n\to K^-\pi^-p$ are defined as follows: $S_{Kp}=(K_{\text{out}}^-+p)^2$, $t_{KK}=(K_{\text{out}}^--K_{\text{in}})^2$, etc. The Treiman-Yang angle in the rest frame of the boson combination was $\phi=\cos^{-1}[(\hat{K}_{\text{in}}\times\hat{K}_{\text{out}}^-)\cdot(\hat{n}\times\hat{K}_{\text{in}}^-)]$, and for the proton-meson combinations $\phi=\cos^{-1}[(\hat{n}\times\hat{p})\cdot(\hat{K}_{\text{in}}^-\times\hat{n})]$. Scattering angle, $\theta_{K\pi}=\cos^{-1}(\hat{K}_{\text{in}}^-\cdot\hat{K}_{\text{out}}^-)$.

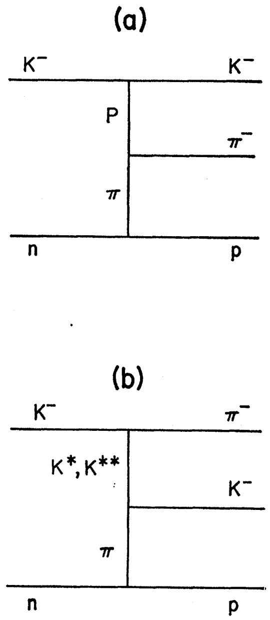

FIG. 5. Double-peripheral diagrams.

Here, $G_\pi(t_{np})$ is the product of the Reggeized pion propagator, its signature factor, and the reduced residue function describing its coupling to the np vertex. Similarly, $G_P(t_{KK})$ refers to the Pomeranchukon and its coupling to the KK vertex, $G_{K^*}(t_{K\pi})$ to the K^* at the $K\pi$ vertex, and $G(t_1,t_2,\omega_T)$ involves the coupling of the two trajectories at the middle vertices. The Toller rotation angle is denoted by ω_T; S_{10} and S_{20} (set to be 1 GeV^2) are scale constants, and C_a and C_b are the normalization constants to be adjusted in fitting the data.

The pion trajectory was assumed to be linear, $\alpha_\pi=\alpha_\pi'(t_{np}-m_\pi^2)$, with slope $\alpha_\pi'=1.2\ (\text{GeV}/c)^{-2}$.[14] It should be noted that, in the limit $t_{np}\to m_\pi^2$, $G_\pi(t_{np})$ must approach the one-pion-exchange (OPE) form:

$$|G_\pi(t_{np})|^2 \to t_{np}/(t_{np}-m_\pi^2)^2.$$

Thus $G_\pi(t_{np})$ was written as the product of the Reggeized propagator, signature factor, and the vertex function $(-t_{np})^{1/2}$ [15]:

$$G_\pi(t_{np})=\pi\alpha_\pi'(-t_{np})^{1/2}(1+e^{-i\pi\alpha_\pi})/2[\sin\pi\alpha_\pi \times\Gamma(\alpha_\pi+1)]. \quad (3)$$

This expression differs from that used in some other analyses[2,4] in which the term $(-t_{np})^{1/2}$ was discarded. The $(-t)^{1/2}$ term is preferable on analyticity grounds and we find support for it in our data.

The K^* trajectory used was $\alpha_{K^*}=(t_{K\pi}-m_{K^*}^2+1)\alpha_{K^*}'$, where $\alpha_{K^*}'=1.0(\text{GeV}/c)^{-2}$ and $m_{K^*}=0.892$ GeV. As shown in Fig. 5(b), one or both of $K^*(890)$ and $K^{**}(1420)$ Regge trajectories can be exchanged in diagram 5(b). Thus the signature factor of each K^* is written $[1+(-1)^J e^{-i\pi\alpha_{K^*}}]/\sin\pi\alpha_{K^*}$, where J is the spin of the K^* considered. However, consideration based on the absence of exotic $K\pi$ resonances and the duality argument lead to exchange degeneracy of (K^*,K^{**}) resulting in a simple, real form of the residue function

$$G_{K^*}(t_{K\pi})=2/[\sin\pi\alpha_{K^*}\,\Gamma(\alpha_{K^*})].$$

The Pomeranchukon was taken to be a fixed pole, $\alpha_P\equiv1$, and $G_P(t_{KK})$ was parametrized as $G_P(t_{KK}) =ie^{\Lambda t_{KK}/2}$ with the slope parameter Λ to be adjusted. Since the DRM does not make any prediction about the dependence of $G(t_1,t_2,\omega_T)$ on the kinematic variables, we assumed it to be constant and absorbed it into the normalization constant.

Resonance production is already weak in our reaction and was reduced to negligible proportions by imposing a cut on the momentum transfer to the nucleon. This cut also enhances the contributions of both diagrams considered here and makes this reaction particularly suitable for explanation in terms of a DRM.

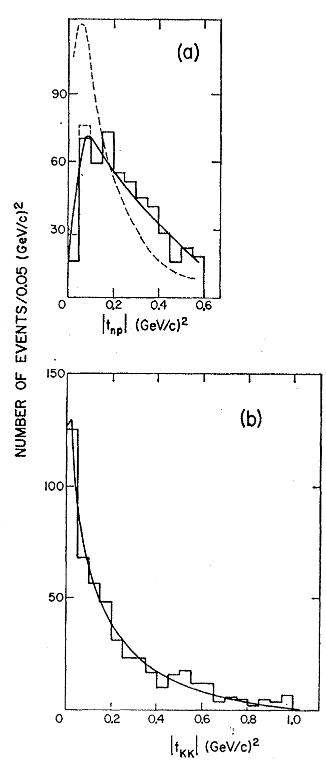

FIG. 6. Invariant momentum transfer distributions for those events associated with diagram 5(a). (a) t_{np} distribution and (b) t_{KK} distribution. The dashed histogram includes the correction mentioned in the text. The dashed line is the prediction of the DRM without the term $(-t_{np})^{1/2}$ in the residue function.

[14] It was found that values of α_π' between 0.8 and 1.2 do not change the fit appreciably.

[15] The term $(-t_{np})^{1/2}$ in the residue function ensures that it will vanish at $t_{np}=0$, as required by OPE. Similar zeros have been introduced into Regge residues in existing analyses of two-body and three-body data. See W. R. Frazer et al., Phys. Rev. Letters 20, 518 (1968) and also Ref. 4.

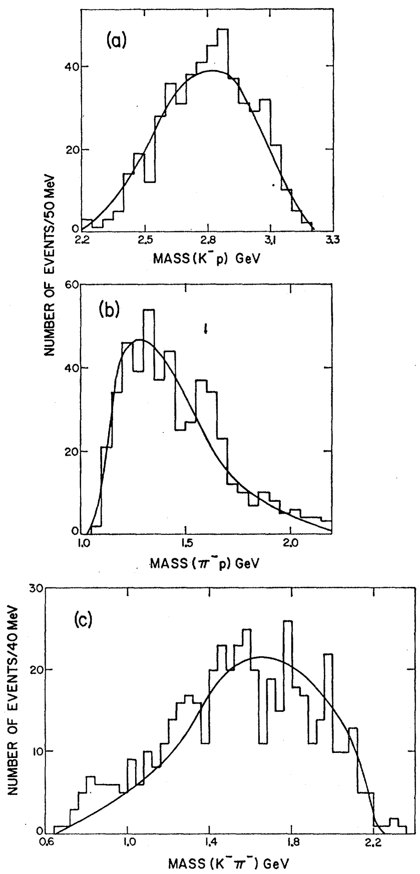

FIG. 7. Invariant mass distributions for diagram 5(a). (a) $M(K^-p)$; (b) $M(p\pi^-)$; and (c) $M(\pi^-K^-)$.

IV. APPLICATION TO DATA

The method of comparing the predictions of the model with the data was to use a Monte Carlo generation of phase-space events weighted by the square of the DRM matrix element. In this way it is possible to include any kinematic cuts and to examine all kinematic variables. A further refinement used was to fold in the spread in c.m. energy for the reaction introduced by the Fermi momentum of the target neutron.[16]

Because the OPE mechanism is dominant only for small momentum transfer, we introduced a cut $|t_{np}| \leqslant 0.6(\mathrm{GeV}/c)^2$ for both the data and for the events generated by the Monte Carlo calculation. About 700 events survived this cut and where divided into three groups depending on the value of the Van Hove angle ω:

(i) for $75° \leqslant \omega \leqslant 130°$ corresponding to diagram 5(a),
(ii) for $150° \leqslant \omega \leqslant 210°$ corresponding to diagram 5(b),
(iii) $130° < \omega < 150°$ for the overlap region.

Events belonging to the first two categories were fitted in terms of the corresponding diagrams, which then fixes the two normalization constants C_a and C_b. Using these values of C_a and C_b and the value of the parameter Λ obtained from diagram 5(a), we then proceeded to predict the over-all distributions.

First we discuss the 450 events associated with diagram 5(a). Events were generated using the matrix element of Eq. (2a), normalized to the observed number of events and all kinematic variables were then projected and compared with the data. Figure 6 shows the t_{np} and t_{KK} distributions. The dashed histogram includes the correction estimated for possible loss due to the deuteron target effect mentioned earlier. The dotted curve in Fig. 6(a) is calculated without the $(-t_{np})^{1/2}$ factor and clearly disagrees with the data. A similar conclusion has been reached by other authors.[15] A suitable value for the slope parameter Λ is found to be

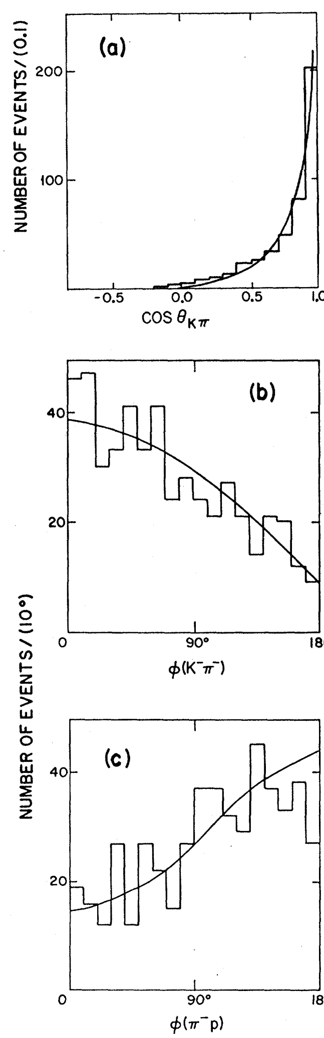

FIG. 8. Distributions of scattering angle and Treiman-Yang angles for diagram 5(a). (a) $K^-\pi^-$ Gottfried-Jackson angle, (b) Treiman-Yang angle in the $K^-\pi^-$ rest frame, and (c) Treiman-Yang angle in the π^-p rest frame. The angles are defined in Ref. 13.

[16] The spread of the total c.m. energy due to the Fermi motion of neutron was $\sim$400 MeV.

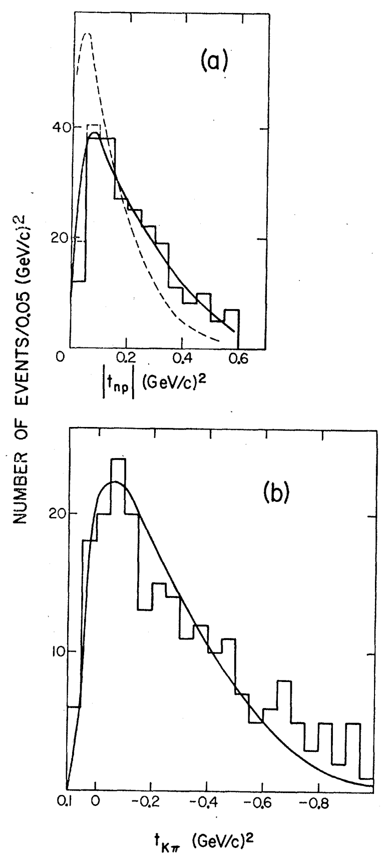

FIG. 9. Invariant momentum transfer distributions for diagram 5(a). (a) t_{np} and (b) $t_{K\pi}$.

5 (GeV/c)$^{-2}$, which is a predicted value of the slope of $K\pi$ elastic-diffraction peak from a factorization method.[17] Figure 7 shows the invariant mass distributions of K^-p, π^-p, and $K^-\pi^-$ combinations. The broad enhancement in the π^-p system near threshold and the preference for high subenergy in the K^-p and $K^-\pi^-$ systems are typical features of double-peripheral models. A peak around 1.6 GeV in the π^-p mass spectrum indicated in Fig. 7(b) may indicate production of an $I=\frac{1}{2}$ N^* by diffraction dissociation of the neutron.

A sharp forward peaking of the $K^-\pi^-$ scattering angular distribution in the Gottfried-Jackson frame is shown by Fig. 8(a). This distribution also shows that selecting events on the basis of the Van Hove angle ω between 75° and 130° corresponds to forward $K^-\pi^-$ scattering. The distribution of the Treiman-Yang angle for the $K^-\pi^-$ system is shown in Fig. 8(b). As previously stressed by Berger, the peak in this distribution near 0° is characteristic of Reggeized pion exchange. We note that a similar Monte Carlo calculation that we have done using the OPE-Deck model[18] provided a good description of the data except for the Treiman-Yang angle, where an isotropic distribution was predicted. The distribution of the Treiman-Yang angle in the π^-p rest frame is shown in Fig. 8(c). The generated distributions were found to be rather insensitive to variations of the Regge parameters α_π' and S_{10}.[14]

We next consider the 190 events associated with diagram 5(b). Because the normalization constant in Eq. (2b) is the only unknown, the quantities shown in Figs. 9–11 are direct predictions of the DRM normalized to the observed number of events. The t_{np} and $t_{K\pi}$ distributions are shown in Fig. 9. The nucleon momentum transfer distribution again demonstrates the need for the term $(-t_{np})^{1/2}$. The $dN/dt_{K\pi}$ shown in Fig. 9(b) vanishes at $t_{K\pi}\sim 0.1$ (GeV/c)^2. This is due to the fact that the phase space vanishes when $t_{K\pi}$ approaches its kinematic limit. In contrast to the events assigned to diagram 5(a), the low-mass enhancement is now in the K^-p system, while the high-mass preference occurs in the π^-p system as seen in Fig. 10. The contamination of this sample of events by a small amount ($\sim$10%) of $Y^*(1520)$ and $Y^*(1820)$ production is indicated in the K^-p mass spectrum in Fig. 10(a). In Fig. 11(a) we show the $K^-\pi^-$ scattering angular distribution seen in the Gottfried-Jackson system. The

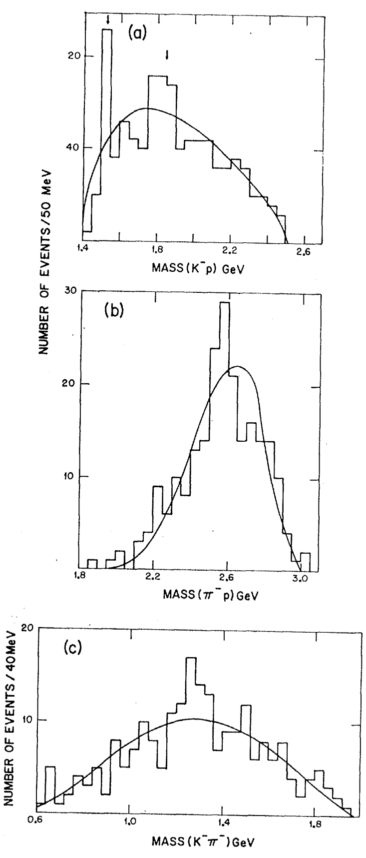

FIG. 10. Invariant mass distributions for diagram 5(b). (a) $M(K^-p)$, (b) $M(\pi^-p)$, and (c) $M(K^-\pi^-)$.

[17] See Ref. 14 of Ref. 6.

[18] For the OPE calculation, the matrix element used was $|M|^2=t_{np}(t_{np}-m_\pi^2)^{-2}[S_{k\pi}-(m_p+m_\pi)^2][S_{k\pi}-(m_p-m_\pi)^2]e^{5t_{KK}}$.

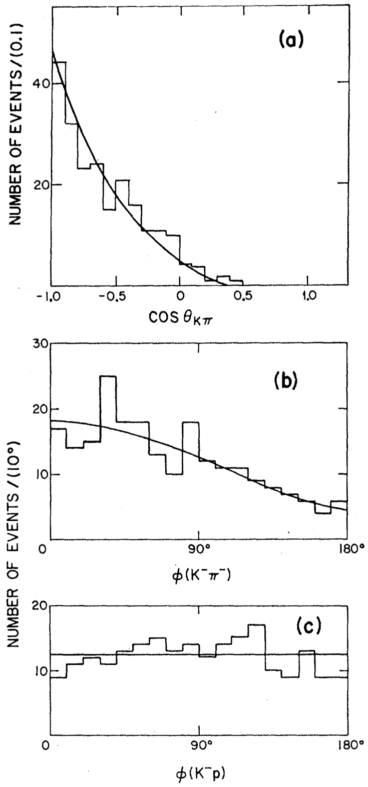

FIG. 11. Distribution of scattering angle and Treiman-Yang angles for diagram 5(b). (a) $K^-\pi^-$ scattering angle, (b) ϕ in the $K^-\pi^-$ system, and (c) ϕ in the K^-p system.

events of this sample belong to backward $K^-\pi^-$ scattering as indicated by this distribution. Again, the experimental distribution of the Treiman-Yang angle computed in the $K^-\pi^-$ rest frame is not uniform. The Treiman-Yang angle associated with K^* exchange and computed in the K^-p rest frame is isotropic. However, the data suggest an anisotropic component, as might be expected for vector-exchange spin-flip coupling. The distributions of these angles are shown in Fig. 11.

Having determined the adjustable parameters, we now study the over-all behavior of the DRM amplitudes for the combined sample (i), (ii), and (iii). The technique is to generate Monte Carlo events using the sum of matrix elements given by Eqs. (2a) and (2b), and to compare this with the data.[19] The selection criteria for both the Monte Carlo events and for the data were $|t_{np}| \leqslant 0.6(\text{GeV}/c)^2$ and $75° \leqslant \omega \leqslant 210°$. The ratio C_b/C_a was found to be 0.4 and the comparisons between the data and the model are shown in Figs. 12–15. The distributions of momentum transfers t_{np}, t_{KK}, and $t_{K\pi}$ are shown in Fig. 12. The dashed histogram in the t_{np} distribution includes the correction for the suppression in the small momentum transfer region due to the exclusion principle. Figure 13(a) shows the invariant mass distribution of the K^-p system. As previously stressed, a negligible amount of resonance production is present in the K^-p system after imposing the momentum transfer cut. The subenergy distribution of the π^-p combination is shown in Fig. 13(b), and as seen in Fig. 13(c), there is no structure in the $K^-\pi^-$ invariant mass distribution. In Fig. 14, we show the distributions of Treiman-Yang angles in the $K^-\pi^-$, π^-p, and K^-p rest frames. The need for Reggeized pion exchange is clearly indicated by the distribution of the Treiman-Yang angle for the $K^-\pi^-$ system. Finally we show the distribution of the Van Hove angle. The unweighted distribution in ω is shown in Fig. 15(a), and the distribution in this angle weighted by the inverse of phase space is shown in Fig. 15(b). The estimated range of ω for the $Y^*(1520)$ and $Y^*(1820)$ is indicated in Fig. 15(a).

[19] Since the matrix element for diagram 5(a) is pure imaginary due to the P exchange, and that for diagram 5(b) is pure real due to the exchange degeneracy, no interference between the two diagrams is expected.

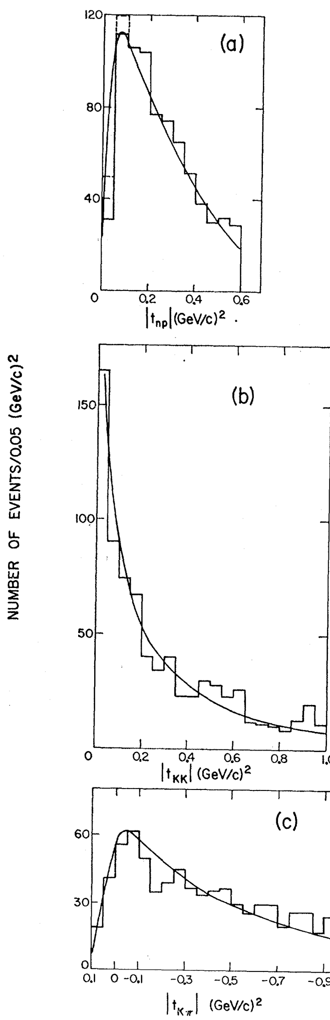

FIG. 12. Momentum transfer distributions for all events with $|t| \leqslant 0.6$ (GeV/c)^2. (a) t_{np}, (b) $t_{K\pi}$. The dashed histogram in (a) includes the correction mentioned in the text.

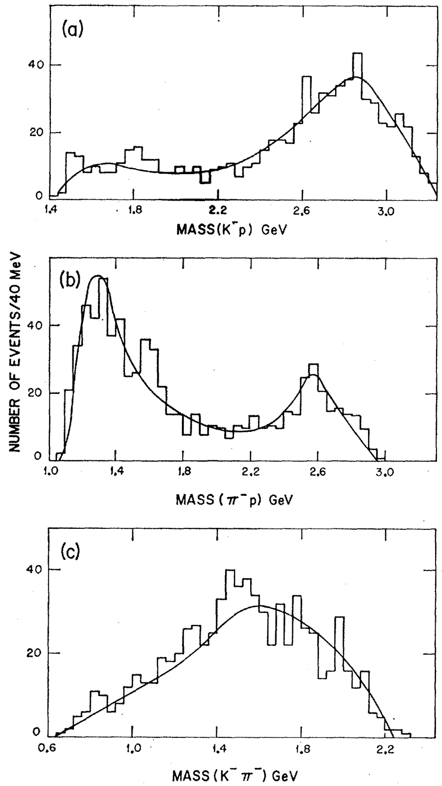

FIG. 13. Invariant mass distributions for all events with $|t| \leq 0.6$ $(\mathrm{GeV}/c)^2$. (a) $M(K^-p)$, (b) $M(\pi^-p)$, and (c) $M(K^-\pi^-)$.

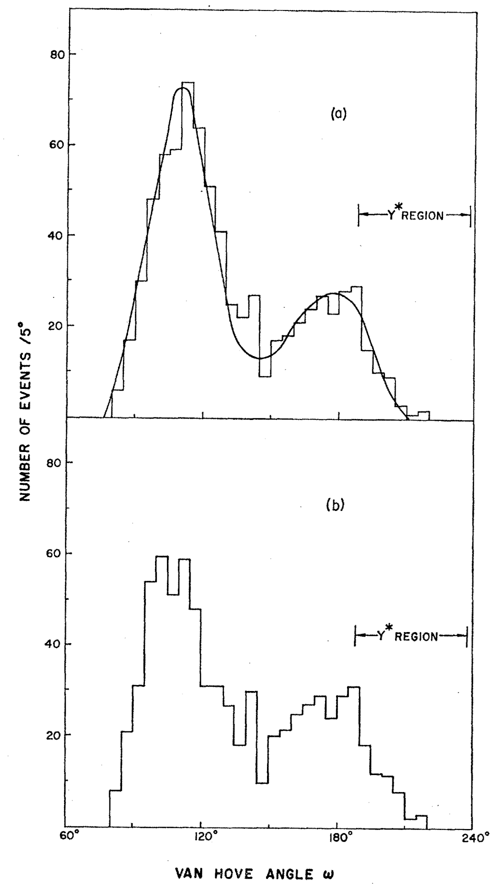

FIG. 15. Distributions of Van Hove angle (a) unweighted and (b) weighted by the inverse of phase space. The arrows indicate the range in ω affected by possible Y^* production.

V. SUMMARY

We have studied the process $K^-n \rightarrow K^-\pi^-p$ at 5.5 GeV/c, in which no strong resonance production is observed. The analysis describes the reaction amplitudes in terms of a double-Regge-pole model. To this extent, it was found that two sets of double-Reggeon exchanges dominate the reaction. One set comprises pion exchange at the nucleon vertex and Pomeranchuk exchange at the boson vertex, and the other consists of π exchange at the nucleon vertex and K^* (K^{**}) exchange at the other vertex. Association of events with the appropriate pair of exchanges was made using the Van Hove plot. Adjustable parameters were the slope of the Pomeranchuk residue function and a normalization constant for each pair of exchanges. The fit was found to be insensitive to any reasonable variations of other Regge parameters such as the scale constant and the slope of the pion trajectory.

Even at this low energy, the DRM gives a good description of the data, in particular, of the Treiman-Yang angle associated with pion exchange. The necessity of a factor $(-t_{np})^{1/2}$ in the pion-nucleon vertex function for the present data is shown by the t_{np} distributions. This contrasts with some other data where this factor was not required.

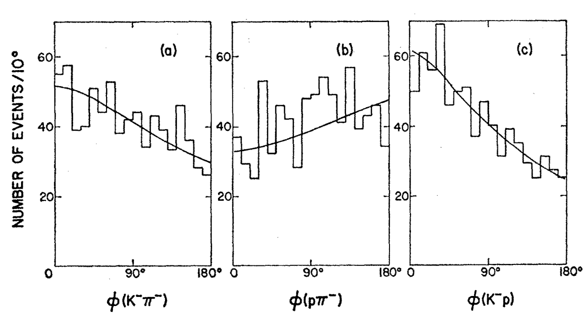

FIG. 14. ϕ distribution for all events with $|t| \leq 0.6$ $(\mathrm{GeV}/c)^2$. (a) in the $K^-\pi^-$ rest frame, (b) π^-p rest frame, and (c) K^-p rest frame.

ACKNOWLEDGMENTS

We thank the staff and crews of the ZGS and 30-in. bubble chamber for their assistance with the exposure. We also thank E. Berger for helpful discussions. The efforts of our scanning, measuring, and data-handling personnel are gratefully acknowledged.